

Malaria Elimination Transmission and Costing in the Asia-Pacific: a multi-species dynamic transmission model

Supplementary File 1: Mathematical model description

Sheetal Silal^{1,2,3} & Lisa White^{2,4}

¹ Modelling and Simulation Hub, Africa (MASHA), Department of Statistical Sciences, University of Cape Town, University of Cape Town, Rondebosch, Cape Town 7700, South Africa

² Centre for Tropical Medicine and Global Health, Nuffield Department of Medicine, University of Oxford, Oxford, UK

³ South African DST-NRF Centre of Excellence in Epidemiological Modelling and Analysis, Stellenbosch University, Cape Town, South Africa

⁴ Mahidol Oxford Tropical Medicine Research Unit, Faculty of Tropical Medicine, Mahidol University, Bangkok, Thailand

This document provides a description of the methodology, equations and parameters underlying the mathematical model for *P. falciparum* and *P. vivax* malaria transmission.

Plasmodium falciparum sub-model

We use a compartmental model for the transmission of *P. falciparum* malaria. It's structure is similar to previously published models [1-6]. There are four infection classes in this model representing infections that are: severe; clinical; asymptomatic and detectable by microscopy; asymptomatic and undetectable by microscopy. Each infection class has a distribution of parasitaemia associated with it that is used to estimate the sensitivity of various diagnostic tests. Each infection class also has an infectiousness associated with it based on infectivity data. The probability of individuals entering each class of infection is dependent on their immunity status. We assume that untreated individuals will transition from higher to lower severity infection classes as they recover and that they can be boosted to higher severity classes on superinfection. We assume that treated individuals test positive for HRP2 after clearance of asexual parasitaemia for different durations depending on the detection limit of the test used. We use a spatially explicit version of this model to estimate the relative contribution of spatially heterogeneous interventions in a spatially heterogeneous transmission setting. The population is divided into a number of interconnected patches with each patch having its own transmission intensity. The patches are connected spatially such that the risk of infection of an individual in a particular patch from an individual in another patch is negatively correlated with the distance between the villages and positively correlated with the population size of the village. This connectivity between villages is used as a proxy for population movement between villages.

The system is depicted in Figure 1 and described by the following set of ordinary differential equations with compartment descriptions in Table 1:

$$\frac{dS}{dt} = \mu P(t) - \mu S - \Lambda(t)S + \omega R$$

$$\frac{dI_n}{dt} = -\mu I_n + p_{sn}(1 - p_s)\Lambda(t)S - r_n I_n + r_a I_a - (1 - p_{rn})(1 - p_r)\Lambda(t)I_n - p_r \Lambda(t)I_n + p_{rn}(1 - p_r)\Lambda(t)(R + H)$$

$$\begin{aligned} \frac{dI_a}{dt} = & -\mu I_a + (1 - p_{sn})(1 - p_s)\Lambda(t)S + (1 - p_{sev})r_c I_c - r_a I_a + (1 - p_{rn})(1 - p_r)\Lambda(t)I_n - p_r \Lambda(t)I_a + \\ & (1 - p_{rn})(1 - p_r)\Lambda(t)(R + H) + ptf(1 - ptf c)r_t(T_o + T_v + T_h) \end{aligned}$$

$$\begin{aligned} \frac{dI_c}{dt} = & -\mu I_c + (1 - \tau)p_s \Lambda(t)S + (1 - \tau_{sev})(1 - \theta_1)r_s I_s - (1 - p_{sev})r_c I_c - p_{sev}r_c I_c + \\ & p_r(1 - \tau)\Lambda(t)(I_n + I_a + R + H) + ptf(ptf c)(1 - ptf tr)r_t(T_o + T_v + T_h) \end{aligned}$$

$$\frac{dI_s}{dt} = -\mu I_s - (1 - \tau_{sev})r_s I_s - \tau_{sev}r_Q I_s + p_{sev}r_c I_c$$

$$\frac{dT_o}{dt} = -\mu T_o + \tau_o p_s \Lambda(t)S - (1 - ptf)r_t T_o + p_r \tau_o \Lambda(t)(I_n + I_a + R + H)$$

$$\frac{dT_v}{dt} = -\mu T_v + \tau_v p_s \Lambda(t)S - (1 - ptf)r_t T_v + p_r \tau_v \Lambda(t)(I_n + I_a + R + H)$$

$$\frac{dT_h}{dt} = -\mu T_h + \tau_h p_s \Lambda(t)S - (1 - ptf)r_t T_h + p_r \tau_h \Lambda(t)(I_n + I_a + R + H) + ptf(ptf c)(ptf tr)r_t(T_o + T_v + T_h)$$

$$\frac{dR}{dt} = -\mu R + r_n I_n - \Lambda(t)R - \omega R + \chi H$$

$$\frac{dH}{dt} = -\mu H + (1 - ptf)r_t(T_o + T_v + T_h) + \tau_{sev}(1 - \theta_2)r_Q I_s - \Lambda(t)H - \chi H$$

where

$$P = S + I_n + I_a + I_c + I_s + T_o + T_v + T_h + R + H$$

$$\Lambda(t) = (1/\lambda(t) + 1/\gamma_h + 1/\gamma_m)^{-1}$$

$$\lambda(t) = seas(t) \frac{b^2 \epsilon_h \epsilon_m \frac{M}{P(t)} I(t)}{(b \epsilon_h \frac{M}{P(t)} + \delta_m) (\frac{\gamma_m}{\gamma_m + \delta_m})}$$

$$I(t) = \frac{\zeta_n I_n(t) + \zeta_a I_a(t) + I_c(t) + I_s(t)}{P(t)}$$

$$seas(t) = 1 + eln * a * \cos(2\pi(t - \phi))$$

$$\tau = \tau_o + \tau_v + \tau_h$$

where eln is the Bivariate ENSO (El Niño southern oscillation) index time series standardised between 0 and 1 and smoothed with a running median to estimate effect size. (Accessible at: <http://www.esrl.noaa.gov/psd/data/climateindices/>).

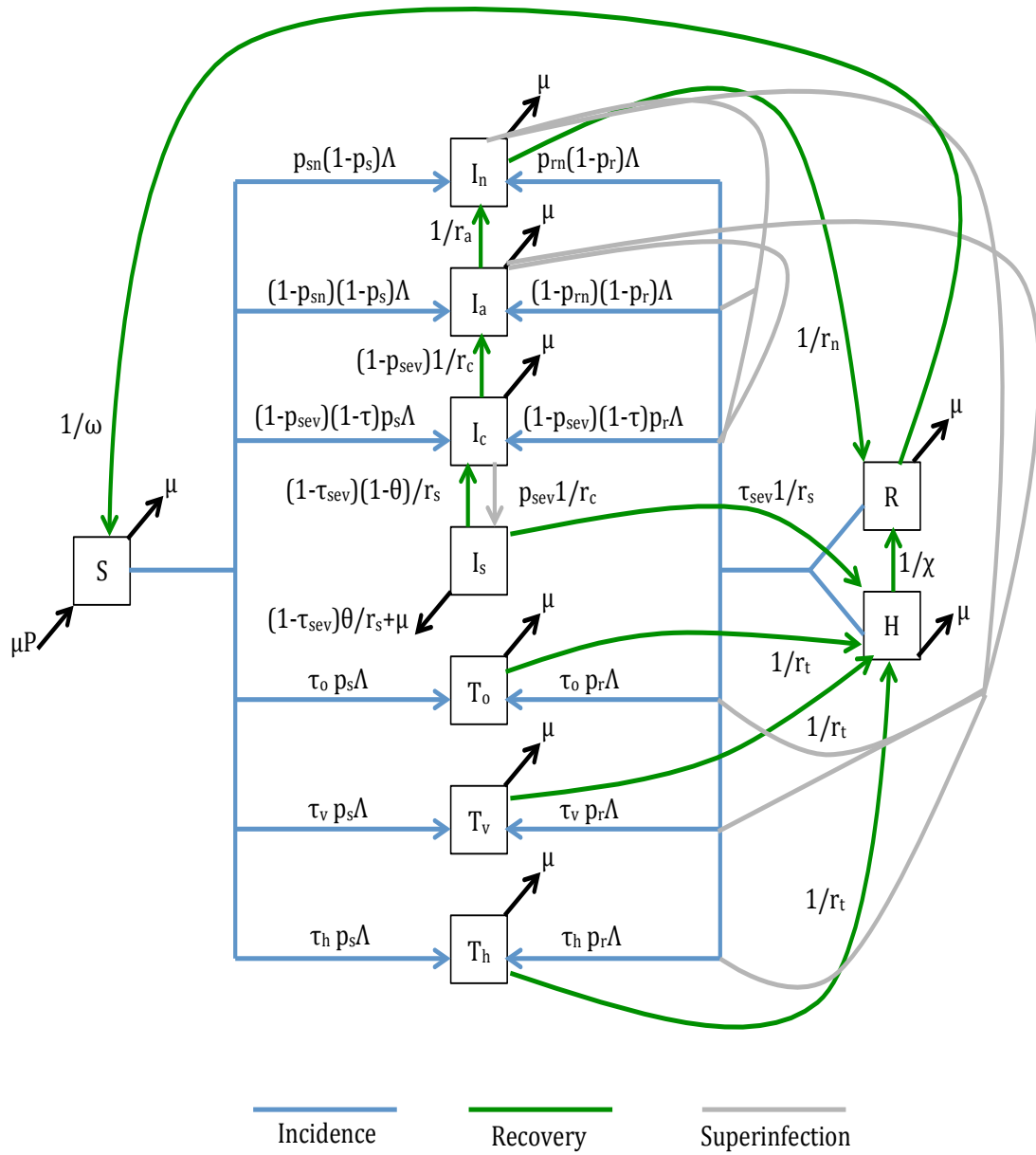


Figure 1 *Plasmodium falciparum* model flow diagram

Plasmodium vivax sub-model

We also use a compartmental model for the transmission of *P. vivax* malaria. Its structure is similar to the *P. falciparum* model with respect to the four infection classes, though there are key differences between the two model structures. *P. vivax* infections are characterized by relapses of malaria arising from persistent liver stages of the parasite (hypnozoites). We assumed that infections may clear with the persistence of hypnozoites in the liver (dependent on a probability) and that these hypnozoites may trigger relapses of infection. The relationship between Glucose 6-phosphate dehydrogenase deficiency (G6PDd) and *P. vivax* malaria is captured in the following manner. The distribution of G6PDd in each patch is determined by available data [7]. The probability of individuals entering each class of infection is dependent on their immunity status. The G6PDd proportion of the population has a reduced probability of clinical infection compared to the non-G6PDd proportion of the population. When primaquine treatment is introduced, those diagnosed with *P. vivax* can receive a test for G6PDd and are given Primaquine depending on the test outcome subject to test sensitivity. As with the *P. falciparum* model, we assume that untreated individuals will transition from higher to lower severity infection classes as they recover and that they can be boosted to higher severity classes on superinfection. The model is also spatially explicit with interconnected patches representing geographic areas of interest.

The system is depicted in Figure 2 and described by the following set of ordinary differential equations with compartment descriptions in Table 1:

Dependencies between *P. vivax* and *P. falciparum* models

The *P. vivax* and *P. falciparum* models are independent models for the same population. The models are entangled together at each time step to incorporate interactions and dependencies between the two species in the following manner:

1. Dual treatment (Treatment of mixed infection)

The untreated population infected with *P. falciparum* malaria who are simultaneously infected with and being treated with a drug for *P. vivax* malaria that is also effective against *P. falciparum* malaria (e.g. ACT, Chloroquine), will also be cured of their *P. falciparum* malaria. Likewise, treatment for a *P. falciparum* infection such as ACT, will also cure a *P. vivax* infection, though hypnozoites may persist in the liver after infection. [8, 9]

2. Triggering

It has been observed in many studies that clinical *P. falciparum* infections are often followed by *P. vivax* infection [10-12]. It has been hypothesized that the subsequent appearance of *P. vivax* implies that a *P. falciparum* episode reactivates *P. vivax* hypnozoites [10]. This is incorporated into the model with the population experiencing a clinical *P. falciparum* infection having a higher probability of *P. vivax* relapse compared to the rest of the population.

3. Radical cure

Primaquine is currently the only available drug that prevents relapse of *P. vivax* malaria. However, Primaquine is dangerous for individuals with G6PD deficiency and should not be used as radical cure for *P. vivax* infections without knowledge of G6PD status [13]. The model assumes that the population is screened for G6PDd and only those who test as G6PD normal (subject to test sensitivity) are given Primaquine.

$$\frac{dS}{dt} = \mu P(t) - \mu S - \Lambda(t)S + \omega R + \kappa L$$

$$\begin{aligned} \frac{dI_n}{dt} = & -\mu I_n + p_{sn}(1-p_s)\Lambda(t)S - r_n I_n + r_a I_a - (1-p_{rn})(1-p_r)\Lambda(t)I_n - p_r \Lambda(t)I_n + p_{rn}(1-p_r)p_{rel}\nu L \\ & + p_{rn}(1-p_r)\Lambda(t)(R+L) \end{aligned}$$

$$\begin{aligned} \frac{dI_a}{dt} = & -\mu I_a + (1-p_{sn})(1-p_s)\Lambda(t)S + (1-p_{sev})r_c I_c - r_a I_a + (1-p_{rn})(1-p_r)\Lambda(t)I_n - p_r \Lambda(t)I_a + \\ & (1-p_{rn})(1-p_r)p_{rel}\nu L + (1-p_{rn})(1-p_r)\Lambda(t)(R+L) + p_{tf}(1-ptftr)r_t(T_o + T_v + T_h + T_{oGD} + T_{vGD} + T_{hGD}) \end{aligned}$$

$$\begin{aligned} \frac{dI_c}{dt} = & -\mu I_c + (1-\tau)p_s\Lambda(t)S + (1-\tau_{sev})(1-\theta_1)r_s I_s - (1-p_{sev})r_c I_c + p_r(1-\tau)\Lambda(t)I_a - p_{sev}r_c I_c + p_r(1-\tau)\Lambda(t)I_n + \\ & p_r(1-\tau)p_{rel}\nu L + p_r(1-\tau)\Lambda(t)(R+L) + p_{tf}(1-ptftr)(ptfc)r_t(T_o + T_v + T_h + T_{oGD} + T_{vGD} + T_{hGD}) \end{aligned}$$

$$\frac{dI_s}{dt} = -\mu I_s - (1-\tau_{sev})r_s I_s - \tau_{sev}r_Q I_s + p_{sev}r_c I_c$$

$$\frac{dT_o}{dt} = -\mu T_o + (1-p_{gd})\tau_o p_s \Lambda(t)S - (1-p_{tf})r_t T_o + (1-p_{gd})p_r \tau_o \Lambda(t)(I_n + I_a + R + L) + (1-p_{gd})p_r \tau_o p_{rel}\nu L$$

$$\frac{dT_v}{dt} = -\mu T_v + (1-p_{gd})\tau_v p_s \Lambda(t)S - (1-p_{tf})r_t T_v + (1-p_{gd})p_r \tau_v \Lambda(t)(I_n + I_a + R + L) + (1-p_{gd})p_r \tau_v p_{rel}\nu L$$

$$\begin{aligned} \frac{dT_h}{dt} = & -\mu T_h + (1-p_{gd})\tau_h p_s \Lambda(t)S - (1-p_{tf})r_t T_h + (1-p_{gd})p_r \tau_h \Lambda(t)(I_n + I_a + R + L) + (1-p_{gd})p_r \tau_h p_{rel}\nu L + \\ & p_{tf}(ptftr)(ptfc)r_t(T_o + T_v + T_h) \end{aligned}$$

$$\frac{dT_{oGD}}{dt} = -\mu T_{oGD} + p_{gd}\tau_o p_s \Lambda(t)S - (1-p_{tf})r_t T_{oGD} + p_{gd}p_r \tau_o \Lambda(t)(I_n + I_a + R + L) + p_{gd}p_r \tau_o p_{rel}\nu L$$

$$\frac{dT_{vGD}}{dt} = -\mu T_{vGD} + p_{gd}\tau_v p_s \Lambda(t)S - (1-p_{tf})r_t T_{vGD} + p_{gd}p_r \tau_v \Lambda(t)(I_n + I_a + R + L) + p_{gd}p_r \tau_v p_{rel}\nu L$$

$$\begin{aligned} \frac{dT_{hGD}}{dt} = & -\mu T_{hGD} + p_{gd}\tau_h p_s \Lambda(t)S - (1-p_{tf})r_t T_{hGD} + p_{gd}p_r \tau_h \Lambda(t)(I_n + I_a + R + L) + p_{gd}p_r \tau_h p_{rel}\nu L \\ & + p_{tf}(ptftr)(ptfc)r_t(T_{oGD} + T_{vGD} + T_{hGD}) \end{aligned}$$

$$\begin{aligned} \frac{dR}{dt} = & -\mu R + (1-p_h)(1-p_{tf})r_t(T_o + T_v + T_h + T_{oGD} + T_{vGD} + T_{hGD}) + (1-p_h)\tau_{sev}(1-\theta_2)r_Q I_s \\ & + r_n I_n - \Lambda(t)R - \omega R \end{aligned}$$

5

$$\frac{dL}{dt} = -\mu L + p_h(1-p_{tf})r_t(T_o + T_v + T_h + T_{oGD} + T_{vGD} + T_{hGD}) + p_h\tau_{sev}(1-\theta_2)r_Q I_s - p_{rel}\nu L - \Lambda(t)L - \kappa L$$

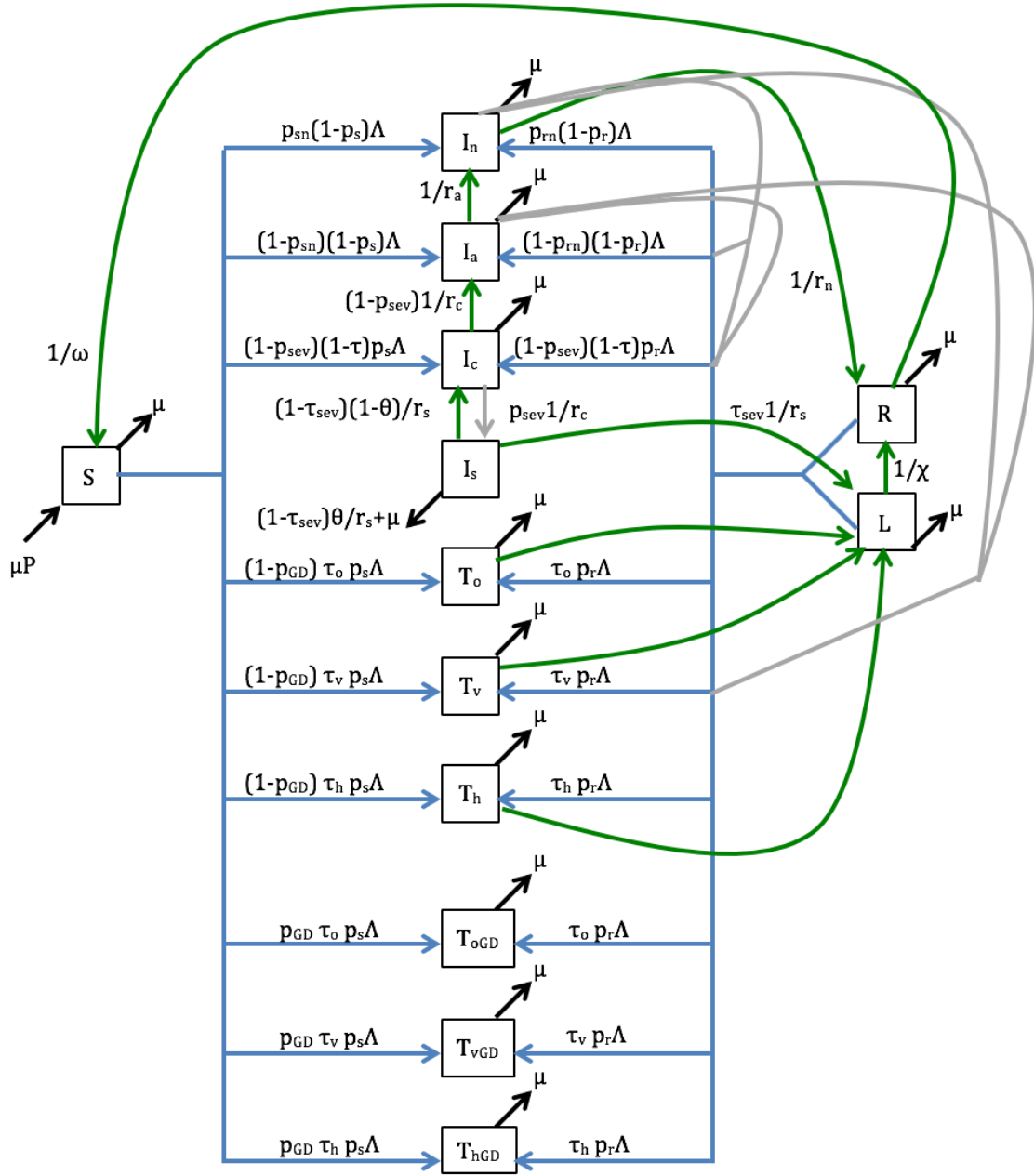


Figure 2 *Plasmodium vivax* model flow diagram

4. Masking

Different brands of Rapid Diagnostic Tests (RDT) have different targets and hence it may be the case that *non-falciparum* malaria is masked by *falciparum* malaria [14]. A comparison of RDTs that are designed to differentiate *falciparum* malaria from *non-falciparum* malaria but cannot differentiate between *non-falciparum* species nor identify *non-falciparum* malaria species within a mixed infection suggested that 11% - 22% of microscopy-confirmed *non-falciparum* cases are missed, with approximately 25% of these cases being declared as positive for *falciparum*. RDTs targeted to detect *P. vivax* specifically, whether alone or part of a mixed infection, were more accurate with tests missing less than 5% of *P. vivax* cases [14]. To account for this it is assumed that 5% of *P. vivax* cases are treated as *P. falciparum* cases and will not be candidates for radical cure in the model.

5. Competition between species

Experiments on patients with mixed infections have suggested that different malaria parasites interact or antagonize each other in the host [15]. The nature of these interactions is not always clearly understood with conflicting clinical results. It appears that though the different malaria species do engage in mutual parasite suppression, which species suppresses which remains unclear. In the case of *P. falciparum* and *P. vivax*, there is evidence for both directions of suppression [16, 17]. With respect with cross immunity, Maitland (1997) suggested the existence of an anti-toxic cross immunity between *P. falciparum* and *P. vivax* while Jeffery (1966) found no evidence for cross immunity [17, 18]. Other studies suggest that mixed infections could be associated with more severe disease [15]. In light of this evidence the model does not account for mutual suppression and cross immunity.

6. Protective effect of G6PDd against malaria

The results of studies examining the risk of malaria for different G6PD-deficient genotypes are not consistent and the nature of protective effect itself is not clearly understood [7, 19]. Leslie (2010) found that study participants with reduced Mediterranean-type G6PD levels were approximately one-fifth as likely to develop *P. vivax* malaria as those with normal G6PD levels while Louicharoen (2009) found that the Mahidol^{487A} variant reduces *vivax*, but not *falciparum* parasite density in humans while having no effect on the number of clinical cases reported [20, 21]. Ruwende et al. (1995) found a reduction in risk for severe *falciparum* malaria in both males and females deficient in the A- G6PD variant while Guindo et al. (2007) found a similar effect in males, but none in females [22, 23]. In light of this evidence the model does not include a protective effect for the G6PDd proportion of the population.

Table 1 Model Variables

Symbol	Definition
<i>Falciparum</i> Variables	
S	Uninfected and non-immune population
H	Uninfected and immune population who test positive by RDT
R	Uninfected and immune population
I_N	Infected and asymptomatic malaria population undetectable by microscopy
I_A	Infected and asymptomatic malaria population detectable by microscopy
I_C	Infected and clinical malaria population
I_S	Infected and severe malaria population
T₀	Population under effective treatment by other means (E.g. Private care)
T_V	Population under effective treatment by Village Malaria Worker
T_H	Population under effective treatment through Health Information System
<i>Vivax</i> Variables	
S	Uninfected and non-immune population
L	Uninfected and immune population with hypnozoites
R	Uninfected and immune population without hypnozoites
I_N	Infected and asymptomatic malaria population undetectable by microscopy
I_A	Infected and asymptomatic malaria population detectable by microscopy
I_C	Infected and clinical malaria population
I_S	Infected and severe malaria population
T₀	Population under effective treatment by other means (E.g. Private care)
T_V	Population under effective treatment by Village Malaria Worker
T_H	Population under effective treatment through Health Information System
T_{0,GD}	Population under effective treatment by other means (E.g. Private care) with G6PDd
T_{V,GD}	Population under effective treatment by Village Malaria Worker with G6PDd
T_{H,GD}	Population under effective treatment through Health Information System with G6PDd

Table 2 Model Parameters

Symbol	Definition	Value	Units	Sim Range	Source
Common Parameters					
M	Maximum populations of mosquitoes		num		estimated from data
ϕ	Month of peak transmission	(1, 12)	month		estimated from data
a	Amplitude of seasonal variation	1	na	(0,1)	assumption
δ_m	Average life expectancy of mosquito	14	days	(10,20)	[24, 25]
b	Number of mosquito bites per human per day	1/3	day ⁻¹	(0.1,0.5)	[26, 27]
ε_m	Probability that a bite from an infectious mosquito will result in infection	50	%	(20,50)	[27-29]
$1/\gamma_M$	Duration of latent period in mosquitoes	10	days	(5, 15)	[13, 24, 30-33]
eff_{IRS}	Effectiveness of indoor residual spraying	25	%	(0, 50)	estimated from data
eff_{ITN}	Effectiveness of bednets	25	%	(0, 50)	estimated from data
hl_{NET}	Half-life of bednets	1.5	year	(1, 2)	[34]
eff_{VMW}	Effectiveness of Village Malaria Worker	60	%	(50, 70)	Expert opinion
eff_{HIS}	Effectiveness of Health Information System	25	%	(10,30)	estimated from data
eff_{OTH}	Effectiveness of other treatment systems	10	%	(5, 15)	estimated from data
$1/\mu$	Average life expectancy of the population	72	year	(68,75)	[35]
eln	Smoothing parameter of el niño effect	21			estimated
Falciparum Parameters					
p_S	Proportion of non-immune individuals expected to develop clinical malaria after infection	90	%	(80,100)	[31, 36]
p_R	Proportion of immune individuals expected to develop clinical malaria after infection	10	%	(0,77)	[37]
p_{SN}	Proportion of non-immune individuals expected to develop sub-patent infection upon challenge	10	%	(0,20)	assumption
p_{RN}	Proportion of immune individuals expected to develop sub-patent infection upon challenge	50	%	(30,70)	assumption
$1/r_S$	Duration of symptoms in an untreated severe infection	10	day	(5,15)	[38, 39]
$1/r_C$	Duration of symptoms in an untreated clinical infection	10	days	(5,15)	[38, 39]
$1/r_A$	Duration of symptoms in an untreated asymptomatic infection	130	days	(60, 200)	[40-42]
τ_{SEV}	Proportion of severe malaria that is treated	80	%	(0, 100)	assumption

p_{sev}	Proportion of clinical infections that become severe	3	%	(5,25)	[43, 44]
ζ_A	Relative infectiousness of asymptomatic infection compared to clinical infection	12.6/27	na	(0,0.50)	[45]
ζ_N	Relative infectiousness of sub-patent infection compared to clinical infection	3.9/27	na	(0., 0.25)	[46]
$1/\omega$	Duration of immunity in an individual without challenge	1	year	(0.5,10)	[41]
θ_1	Probability that untreated severe malaria progresses to death	70	%	(50,80)	[44]
θ_2	Probability that treated severe malaria progresses to death	22	%	(15,30)	[47-49]
ε_h	Probability that a bite from an infectious human will result in infection	50	%	(7,64)	[30, 50]
$1/\gamma_H$	Incubation period and time to gametocytemia in humans	21	days	(14,24)	[30-33, 51]
$1/\chi$	Period of HRP2 detectability by RDT	28	days	(21,37)	[52-54]
$1/r_T$	Time taken to clear asexual parasites after treatment	3	day	(3,7)	[55]
$1/r_Q$	Recovery time with quinine for severe infections	6	days	(4,8)	[56]
ptf	Baseline probability of treatment failure on ACT	5	%	(1,10)	assumption
$ptfc$	Probability of being clinical after treatment failure	0.75	%	(0.5, 0.9)	assumption
$ptftr$	Probability of seeking trt if clinical, after treatment failure	0.27	%	(0.1, 0.4)	Estimated from data
Vivax Parameters					
p_s	Proportion of non-immune individuals expected to develop clinical malaria after infection	90	%	(80,100)	[57]
p_R	Proportion of immune individuals expected to develop clinical malaria after infection	10	%	(0,30)	[58]
p_{SN}	Proportion of non-immune individuals expected to develop sub-patent infection upon challenge	10	%	(0,20)	[57]
p_{RN}	Proportion of immune individuals expected to develop sub-patent infection upon challenge	17	%	(10,40)	[59]
$1/r_s$	Duration of symptoms in an untreated severe infection	5	day	(2,10)	assumption
$1/r_c$	Duration of symptoms in an untreated clinical infection	20	days	(2,60)	[60, 61]
$1/r_A$	Duration of symptoms in an untreated asymptomatic infection	130	days	(60, 200)	[60, 62-64]
τ_{SEV}	Proportion of severe malaria that is treated	80	%	(0, 100)	assumption
p_{sev}	Proportion of clinical infections that become severe	3	%	(5,25)	[44, 65]

ζ_A	Relative infectiousness of asymptomatic infection compared to clinical infection	1	na	(0,0.1)	[66]
ζ_N	Relative infectiousness of sub-patent infection compared to clinical infection	1	na	(0, 1)	[66]
$1/\omega$	Duration of immunity in an individual without challenge	1	year	(0.5,10)	assumption
θ_1	Probability that untreated severe malaria progresses to death	20	%	(5,70)	[44, 67]
θ_2	Probability that treated severe malaria progresses to death	0.02	%	(5,70)	[49, 68-70]
ε_h	Probability that a bite from an infectious human will result in infection	23	%	(7,40)	[13, 28, 71]
$1/\gamma_M$	Duration of latent period in mosquitoes	12	days	(5, 15)	[72, 73]
$1/\gamma_H$	Incubation period and time to gametocytemia in humans	17	days	(15,20)	[13, 51, 74]
$1/r_T$	Time taken to clear asexual parasites in uncomplicated <i>Pf</i> infection with treatment	3	day	(3,7)	[55]
$1/r_Q$	Recovery time with quinine for severe infections	6	days	(4,8)	[56]
ptf	Baseline probability of treatment failure on ACT	5	%	(1,10)	assumption
$ptfc$	Probability of being clinical after treatment failure	0.75	%	(0.5, 0.9)	assumption
$ptftr$	Probability of seeking trt if clinical, after treatment failure	0.27	%	(0.1, 0.4)	Estimated from data
$ptfp$	Probability of treatment failure on Primaquine	10	%	(5, 15)	[75-77]
adh_p	Non-adherence to 14-day self-administered treatment of primaquine	15	%	(10,30)	[78]
$1/r_P$	Duration of Primaquine treatment	14	day	(12,16)	[8, 79]
$1/\kappa$	Hypnozoite death rate	400	day	(330, 500)	[13, 28, 73]
$psens$	Sensitivity of Carestart v2 G6PDd RDT	97	%	(95-100)	[80]
pgd	Probability of a clinical infection if G6PDd	30	%	(0, 100)	[21]
$mask$	Proportion of <i>P. Vivax</i> cases masked as <i>P. falciparum</i> cases	5	%	(5, 25)	[14]
$prel$	Probability of relapse	25	%	(14,29)	[11, 81]
$Incprel$	Probability of relapse due to triggering from a treated <i>P. falciparum</i> case	35	%	(20,47)	[11, 81]
$1/\nu$	Time to first relapse	45	day	(21,50,150)	[13, 28, 73, 82]
ph	Probability of recovering with hypnozoites under ACT	68	%	(50,80)	[13, 83]
$phprim$	Probability of recovering with hypnozoites under Primaquine	13	%	(10,30)	[13, 83]

Sub-patent infection and diagnostics

We assume that parasitaemia (parasites per μl) within each infection class (sub-patent, asymptomatic and clinical) is log-normally distributed as described in [84]. We also use a mixture model approach to obtain the distribution for severe infection using the data from [85].

The following table summarises the model parameters and their sources:

Description	Unit	Pf Value	Ref	Pv Value	Ref
Geometric mean parasitaemia for sub-patent infections (mn_N)	μl^{-1}	5	[86]	5	[86, 87]
Geometric mean parasitaemia for asymptomatic infections (mn_A)	μl^{-1}	5158	[86]	750	
Geometric mean parasitaemia for clinical infections (mn_C)	μl^{-1}	25000	[85, 88]	5000	[89]
Geometric mean parasitaemia for severe infections (mn_S)	μl^{-1}	350000	[85]	20000	[90]
Log standard deviation of log-normal parasite distribution for sub-patent infections	-	0.75		0.75	
Log standard deviation of log-normal parasite distribution for asymptomatic infections	-	1.5	[88, 91]	1.5	[85, 88]
Log standard deviation of log-normal parasite distribution for clinical infections	-	1.3	[85, 88]	1.3	[25, 85]
Log standard deviation of log-normal parasite distribution for severe infections	-	0.26	[85]	4	[25]

The following table describes the detection limits also described in [84]:

Description	Units	Pf Value	Ref
Detection limit for conventional RDT	μl^{-1}	200	[92]
Detection limit for microscopy	μl^{-1}	100	[92]
Detection limit for proposed RDT	μl^{-1}	5	[93, 94]
Detection limit for conventional qPCR	μl^{-1}	0.2	[95]

Test sensitivity:

The parameters above are used to compute diagnostic sensitivity. For each disease class, i , the sensitivity of a test, x , with detection limit, d_T , is given by the formula:

$$sens_{i,x} = 1 - \frac{1}{2} \left[1 + \operatorname{erf} \left(\frac{d_T - \mu_i}{\sigma_i \sqrt{2}} \right) \right]$$

Where μ_i and σ_i are the log-mean and the log-standard deviation of the log-normal distribution of parasitaemia for disease class $i \in \{\text{sub-patent, asymptomatic, clinical, severe}\}$.

Test specificity:

It has been shown that treated individuals remain positive by conventional RDT for approximately 28 days after successful clearance of asexual parasites [52-54]. An H compartment (individuals recently recovered who are not infected but test positive by RDT) has therefore been included in the model in order to simulate this. The duration of time spent in the H compartment is dependent on the sensitivity of the RDT to detect HRP2 which is assumed to be linearly correlated with its asexual parasite detection limit.

Duration in each infection class:

For severe, clinical and asymptomatic infection the duration of infection is well documented. For sub-patent infection, we assume that the duration of sub-patent infection, δ_N , can be extrapolated from the duration of infection of asymptomatic infection, δ_A , and an assumption of log-linear decline in parasitaemia using the following formula:

$$\delta_N = \delta_A \frac{\mu_N - d_0}{\mu_A - \mu_N}$$

Where μ_N is the log-mean of the log-normal distribution of parasitaemia for sub-patent infection, μ_A is the log-mean of the log-normal distribution of parasitaemia for asymptomatic infection and d_0 is the detection limit of the most sensitive test (qPCR). Using the parameters above, we would expect sub-patent infection to be detectable by qPCR for 75 days.

Force of infection and Seasonality

The force of infection on humans, λ is derived by assuming that mosquito dynamics of an SEI model are at a steady state resulting in the following:

$$\Lambda(t) = (1/\lambda(t) + 1/\gamma_h + 1/\gamma_m)^{-1}$$

$$\lambda(t) = seas(t) \frac{b^2 \epsilon_h \epsilon_m \frac{M}{P(t)} I(t)}{(b \epsilon_h \frac{M}{P(t)} + \delta_m) (\frac{\gamma_m}{\gamma_m + \delta_m})}$$

$$I(t) = \frac{\zeta_n I_n(t) + \zeta_a I_a(t) + I_c(t) + I_s(t)}{P(t)}$$

$$seas(t) = 1 + eln * a * \cos(2\pi(t - \phi))$$

where eln is the Bivariate ENSO (El Niño southern oscillation) index time series standardised between 0 and 1 and smoothed with a running median to estimate effect size. (Accessible at: <http://www.esrl.noaa.gov/psd/data/climateindices/>).

Spatial heterogeneity

A spatially explicit version of this multi-species model can be formulated in a metapopulation framework. This enables the estimation of the relative contribution of spatially targeted interventions in a spatially heterogeneous transmission setting. The area/population of interest is divided into a number of interconnected patches with each patch representing a country/sub-population having its own transmission intensity. The patches are connected spatially such that the risk of infection of an individual in a particular patch from an individual in another patch is negatively correlated with the distance between the patches.

The probability of an individual from patch i being in patch j , σ_{ij} , is assumed to be given by:

$$\sigma_{ij} = \left(\frac{1}{1 + \text{het } h_{ij}} \right) / \sum_{j=1}^N \frac{1}{1 + \text{het } h_{ij}}$$

Where h_{ij} is the Euclidian distance between the centroids of patches i and j and N is the number of patches. The parameter, het , is a measure of the level of spatial heterogeneity where $\text{het}=0$ simulates uniform mixing between patches and $\text{het}=\infty$ simulates no mixing between patches.

Then $\sum_{j=1}^N (\sigma_{ji} P_j)$ becomes the “augmented population” of patch i , meaning the population of patch i combined with the parts of the populations of the other patches which are mixing with patch i .

The force of infection on humans, λ , in patch i can be derived by considering a susceptible human from patch i visiting patch j and being bitten there by an infected mosquito and infected before returning to patch i :

$$\lambda = \sum_{j=1}^N \sigma_{ij} \text{seas}_j \left(\frac{b^2 \epsilon_h \epsilon_m \frac{M_j}{P_j}}{(b \epsilon_h \frac{M_j}{P_j} + \delta_m) (\frac{\gamma_m}{\gamma_m + \delta_m})} \times \frac{\zeta_n I_{nj} + \zeta_a I_{aj} + I_{cj} + I_{sj}}{\sum_{j=1}^N \sigma_{ij} P_j} \right)$$

Model Interventions

The table below summarises the impact that each of the interventions modelled has on model parameters/equations.

Intervention	Description	Model Impact
Passive treatment	Treatment probabilities (τ) for different avenues of treatment (v, h, o) dependent on coverage (cov), treatment-seeking and treatment effectiveness (eff) and diagnostic sensitivity (sens)	See below
$\tau_v = \text{cov}_v \times \text{eff}_v \times \text{sens}_v$ $\tau_h = (1 - \text{cov}_v \text{eff}_v) \times \text{eff}_h \times \text{sens}_h$ $\tau_o = (1 - \text{cov}_v \text{eff}_v - (1 - \text{cov}_v \text{eff}_v) \text{eff}_h) \times \text{eff}_o \times \text{sens}_o$		
Long Lasting Insecticide-treated Nets	Net distribution as a proportion of the population at risk (itn) and the half-life of the net (hlnet) are used to compute cumulative coverage (itncov). This, together with usage and ability to prevent	See below

	transmission (<i>itneff</i>) is used to decrease the transmission function λ	
$itncov_t = itn_t + 0.5itncov_{t-1}e^{-\frac{1}{12}/(hlnet)}$ $\lambda_t^* = (1 - itncov_t \times itneff) \times \lambda_t$		
Indoor residual spraying	Number of people protected by IRS as a proportion of the population at risk (<i>irs</i>) and the half-life of the insecticide (<i>hlspray</i>) are used to compute cumulative coverage (<i>irscov</i>). This, together with ability to prevent transmission (<i>irseff</i>) is used to decrease the transmission function λ	See below
$irscov_t = irs_t + 0.5irscov_{t-1}e^{-\frac{1}{12}/(hlspray)}$ $\lambda_t^* = (1 - irscov_t \times irseff) \times \lambda_t$		
Injectable artesunate	Switching from treatment of severe infections with quinine to injectable artesunate	Parameters decreased: 1/r _Q – recovery time pmort – probability of death of treated severe infections
Single dose P.v. treatment	Switching from a 14 day regimen of Primaquine to a 1 day regimen of new treatment.	Parameters affected 1/r _p = recovery time adhr = adherence
New P.f. drug	Switching to a new drug against Pf	Parameter reduced: ptf – probability of treatment failure
Mass Drug Administration	Implementing mass treatment at a coverage (<i>mcov</i>) over a duration of implementation of a single round (<i>mdur</i>) to form a rate of <i>mrte</i> : $mrte = -\ln\left(\frac{1 - mcof}{mdur}\right)$ The protective duration of the drug is given by 1/ <i>mrec</i> .	See below
<p>Addition of the following differential equations to the model structure:</p> $\frac{dSm_f}{dt} = mrte \times S_f - (mrec + \mu)Sm_f$ $\frac{dTm_f}{dt} = mrte \times (P_f - (S_f + H_f + R_f)) - ptf \times mrec \times Tm_f - (1 - ptf)r_t Tm_f - \mu Tm_f$ $\frac{dHm_f}{dt} = mrte \times H_f + (1 - ptf)r_t Tm_f - (mrec + \mu)Hm_f$ $\frac{dRm_f}{dt} = mrte \times R_f - (mrec + \mu)Rm_f$ $\frac{dSm_v}{dt} = mrte \times S_v - (mrec + \mu)Sm_v$ $\frac{dTm_v}{dt} = mrte \times (P_v - (S_v + L_v + R_v)) - ptf \times mrec \times Tm_v - (1 - ptf)r_t Tm_v - \mu Tm_v$		

$$\begin{aligned}\frac{dLm_v}{dt} &= mrate \times L_v + p_h(1 - ptf)r_t Tm_v - (mrec + \mu)Lm_v \\ \frac{dRm_v}{dt} &= mrate \times R_v + (1 - p_h)(1 - ptf)r_t Tm_v - (mrec + \mu)Rm_v\end{aligned}$$

Model calibration

The model was initially calibrated to the reported annual incidence data from the World Malaria Reports using a pseudo Likelihood maximisation approach based on parameter sets being drawn randomly from the simulation ranges specified in Table 2 and with parameter sets with the highest likelihood being selected for the model. The extent of the data were such that while reported distribution of LLINs and IRS were included in the model to inform changes in incidence, there was no data available on health system advances between 2000 and 2015 such as the introduction of community malaria workers etc. These were imputed based on observed changes in reported incidence.

Thus the model was further calibrated to the estimated burden of disease separately for *P. falciparum* and *P. vivax* malaria to capture the variability in the treatment seeking and completeness rates detailed in Maude, Riley [96], Riley and Maude [97].

Figures 3 and 4 depict the observed clinical burden against the model predicted clinical burden for *P. falciparum* and *P. vivax* malaria respectively. While the model captures the general trend of incidence well, it is unsurprising that the historic data is not always replicated. In addition to the limitations described above, the data were collected at a time when a large proportion of malaria cases reported were suspected, rather than confirmed cases and many countries were still using rapid diagnostic tests that were unable to distinguish between malaria species. In light of this, the authors placed more weight on replicating the most recent data well compared to historic data.

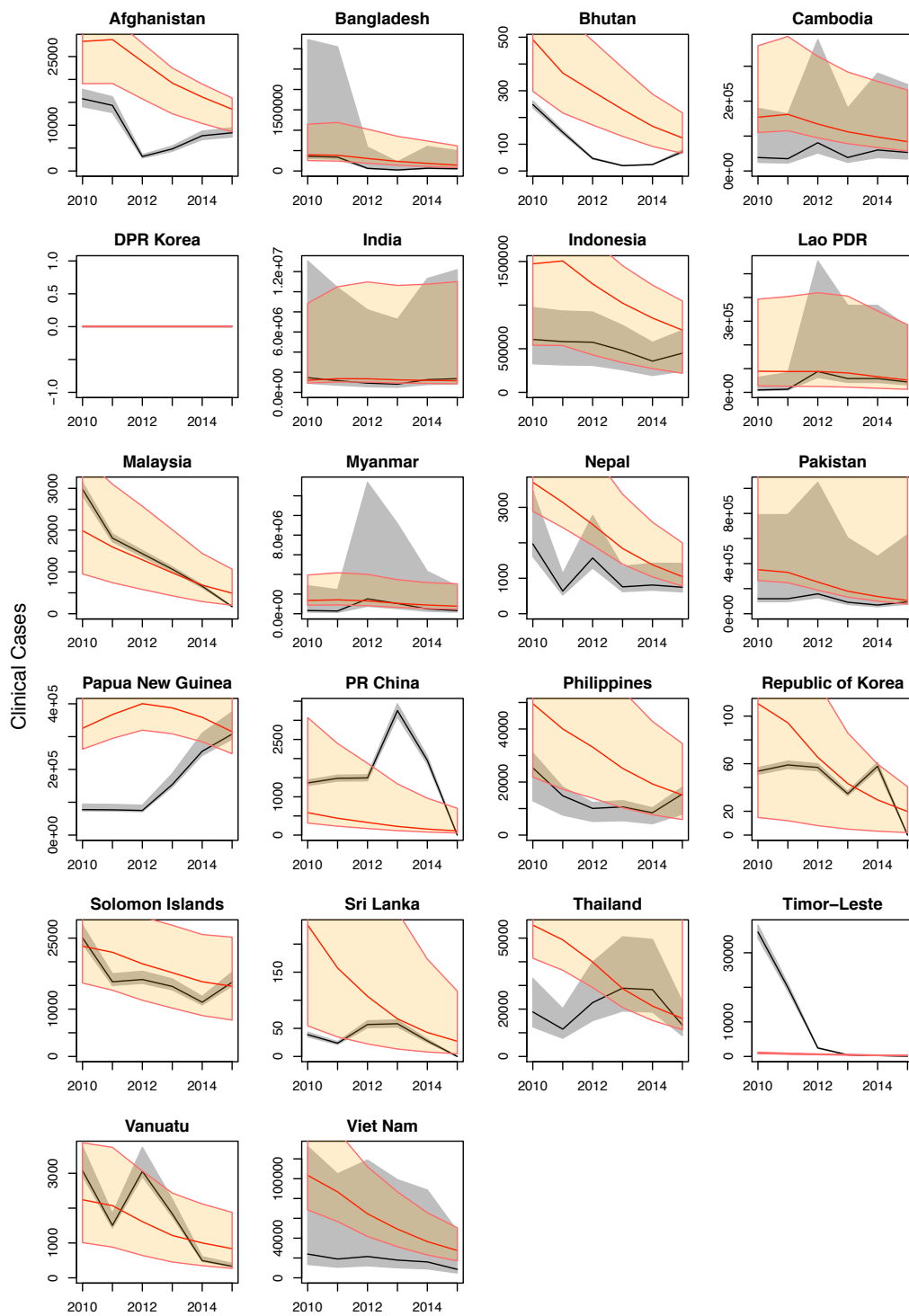


Figure 3 Calibration: *P. falciparum* estimated clinical burden (grey) with predicted clinical burden (red)

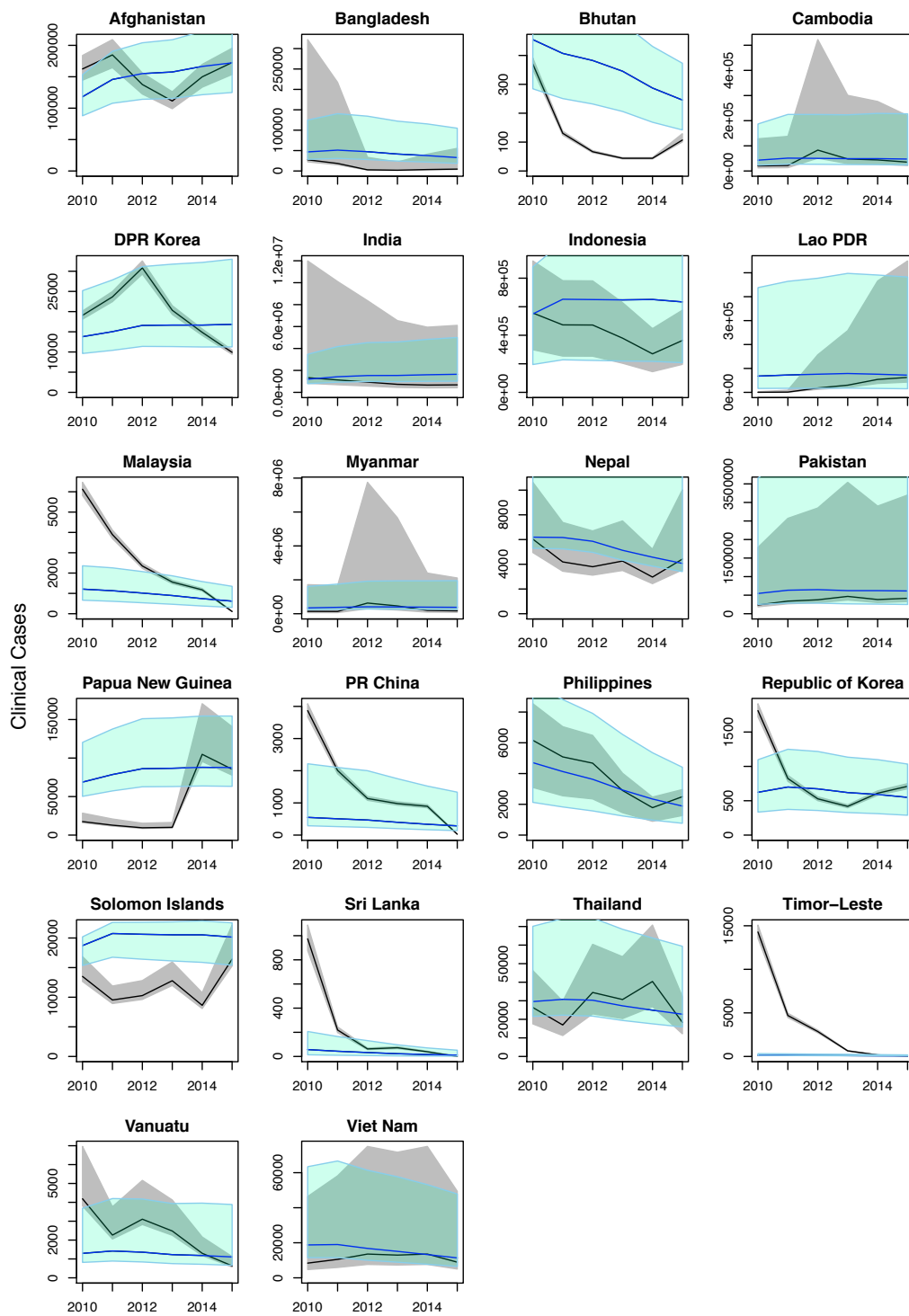


Figure 4 Calibration: *P. vivax* estimated clinical burden (grey) with predicted clinical burden (blue)

References

1. Aguas, R., et al., *Prospects for malaria eradication in sub-Saharan Africa*. PLoS One, 2008. **3**(3): p. e1767.
2. Silal, S.P., et al., *Towards malaria elimination in Mpumalanga, South Africa: a population-level mathematical modelling approach*. Malaria Journal, 2014. **13**(1): p. 297-297.
3. White, L.J., et al., *The role of simple mathematical models in malaria elimination strategy design*. Malar J, 2009. **8**: p. 212.
4. Silal, S.P., et al., *Predicting the impact of border control on malaria transmission: a simulated focal screen and treat campaign*. Malaria Journal, 2015. **14**.
5. Silal, S.P., et al., *Hitting a Moving Target: A Model for Malaria Elimination in the Presence of Population Movement*. PLoS One, 2015. **10**(12): p. e0144990.
6. Slater, H.C., et al., *Assessing the impact of next-generation rapid diagnostic tests on Plasmodium falciparum malaria elimination strategies*. Nature, 2015. **528**(7580): p. S94-101.
7. Howes, R.E., et al., *G6PD deficiency prevalence and estimates of affected populations in malaria endemic countries: a geostatistical model-based map*. PLoS Med, 2012. **9**(11): p. e1001339.
8. White, N.J., *The role of anti-malarial drugs in eliminating malaria*. Malar J, 2008. **7 Suppl 1**: p. S8.
9. Pukrittayakamee, S., et al., *Effects of different antimalarial drugs on gametocyte carriage in P. vivax malaria*. Am J Trop Med Hyg, 2008. **79**(3): p. 378-84.
10. White, N.J., *Determinants of relapse periodicity in Plasmodium vivax malaria*. Malar J, 2011. **10**: p. 297.
11. Lin, J.T., et al., *Plasmodium falciparum gametocyte carriage is associated with subsequent Plasmodium vivax relapse after treatment*. PLoS One, 2011. **6**(4): p. e18716.
12. Snounou, G. and N.J. White, *The co-existence of Plasmodium: sidelights from falciparum and vivax malaria in Thailand*. Trends Parasitol, 2004. **20**(7): p. 333-9.
13. Chamchod, F. and J.C. Beier, *Modeling Plasmodium vivax: relapses, treatment, seasonality, and G6PD deficiency*. J Theor Biol, 2013. **316**: p. 25-34.
14. Abba, K., et al., *Rapid diagnostic tests for diagnosing uncomplicated non-falciparum or Plasmodium vivax malaria in endemic countries*. Cochrane Database Syst Rev, 2014(12): p. Cd011431.
15. Mayxay, M., et al., *Mixed-species malaria infections in humans*. Trends Parasitol, 2004. **20**(5): p. 233-40.
16. Mayxay, M., et al., *Identification of cryptic coinfection with Plasmodium falciparum in patients presenting with vivax malaria*. Am J Trop Med Hyg, 2001. **65**(5): p. 588-92.
17. Maitland, K., T.N. Williams, and C.I. Newbold, *Plasmodium vevax and P. falciparum: Biological interactions and the possibility of cross-species immunity*. Parasitol Today, 1997. **13**(6): p. 227-31.
18. Jeffery, G.M., *Epidemiological significance of repeated infections with homologous and heterologous strains and species of Plasmodium*. Bull World Health Organ, 1966. **35**(6): p. 873-82.
19. Hedrick, P.W., *Population genetics of malaria resistance in humans*. Heredity (Edinb), 2011. **107**(4): p. 283-304.
20. Leslie, T., et al., *The impact of phenotypic and genotypic G6PD deficiency on risk of plasmodium vivax infection: a case-control study amongst Afghan refugees in Pakistan*. PLoS Med, 2010. **7**(5): p. e1000283.
21. Louicharoen, C., et al., *Positively selected G6PD-Mahidol mutation reduces Plasmodium vivax density in Southeast Asians*. Science, 2009. **326**(5959): p. 1546-9.

22. Ruwende, C., et al., *Natural selection of hemi- and heterozygotes for G6PD deficiency in Africa by resistance to severe malaria*. *Nature*, 1995. **376**(6537): p. 246-9.
23. Guindo, A., et al., *X-linked G6PD deficiency protects hemizygous males but not heterozygous females against severe malaria*. *PLoS Med*, 2007. **4**(3): p. e66.
24. Anderson, R.M. and R.M. May, *Infectious diseases of humans: dynamics and control* London. 1991, Oxford: Oxford University Press.
25. Wanji, S., et al., *Anopheles species of the mount Cameroon region: biting habits, feeding behaviour and entomological inoculation rates*. *Trop Med Int Health*, 2003. **8**(7): p. 643-9.
26. Churcher, T.S., J.F. Trape, and A. Cohuet, *Human-to-mosquito transmission efficiency increases as malaria is controlled*. *Nat Commun*, 2015. **6**: p. 6054.
27. Ross, R., *SOME A PRIORI PATHOMETRIC EQUATIONS*. *Br Med J*, 1915. **1**(2830): p. 546-7.
28. Robinson, L.J., et al., *Strategies for understanding and reducing the Plasmodium vivax and Plasmodium ovale hypnozoite reservoir in Papua New Guinean children: a randomised placebo-controlled trial and mathematical model*. *PLoS Med*, 2015. **12**(10): p. e1001891.
29. Smith, D.L., et al., *A quantitative analysis of transmission efficiency versus intensity for malaria*. *Nat Commun*, 2010. **1**: p. 108.
30. Chitnis, N., J.M. Hyman, and J.M. Cushing, *Determining important parameters in the spread of malaria through the sensitivity analysis of a mathematical model*. *Bull Math Biol*, 2008. **70**(5): p. 1272-96.
31. Collins, W.E. and G.M. Jeffery, *A retrospective examination of sporozoite- and trophozoite-induced infections with Plasmodium falciparum: development of parasitologic and clinical immunity during primary infection*. *Am J Trop Med Hyg*, 1999. **61**(1 Suppl): p. 4-19.
32. Eyles, D.E. and M.D. Young, *The duration of untreated or inadequately treated Plasmodium falciparum infections in the human host*. *J Natl Malar Soc*, 1951. **10**(4): p. 327-36.
33. Thompson, D., *A research into the production, life and death of crescents in malignant tertian malaria, in treated and untreated cases, by an enumerative method; the leucocytes in malarial fever: a method of diagnosing malaria long after it is apparently cured*. 1911: University Press.
34. Center for Disease Control. Accessed: 20 January 2015]; Available from: http://www.cdc.gov/malaria/malaria_worldwide/reduction/itn.html.
35. United Nations Statistics Division, *World Statistics Pocketbook*. 2016, United Nations.
36. Griffin, J.T., N.M. Ferguson, and A.C. Ghani, *Estimates of the changing age-burden of Plasmodium falciparum malaria disease in sub-Saharan Africa*. *Nat Commun*, 2014. **5**: p. 3136.
37. Collins, W.E. and G.M. Jeffery, *A retrospective examination of secondary sporozoite- and trophozoite-induced infections with Plasmodium falciparum: development of parasitologic and clinical immunity following secondary infection*. *Am J Trop Med Hyg*, 1999. **61**(1 Suppl): p. 20-35.
38. Griffin, J.T., et al., *Reducing Plasmodium falciparum malaria transmission in Africa: a model-based evaluation of intervention strategies*. *PLoS Med*, 2010. **7**(8).
39. Miller, M.J., *Observations on the natural history of malaria in the semi-resistant West African*. *Trans R Soc Trop Med Hyg*, 1958. **52**(2): p. 152-68.
40. Felger, I., et al., *The dynamics of natural Plasmodium falciparum infections*. *PLoS One*, 2012. **7**(9): p. e45542.

41. Filipe, J.A., et al., *Determination of the processes driving the acquisition of immunity to malaria using a mathematical transmission model*. PLoS Comput Biol, 2007. **3**(12): p. e255.
42. Sama, W., et al., *An immigration-death model to estimate the duration of malaria infection when detectability of the parasite is imperfect*. Stat Med, 2005. **24**(21): p. 3269-88.
43. Griffin, J.T., et al., *Gradual acquisition of immunity to severe malaria with increasing exposure*. Proc Biol Sci, 2015. **282**(1801): p. 20142657.
44. Lubell, Y., et al., *Likely health outcomes for untreated acute febrile illness in the tropics in decision and economic models; a Delphi survey*. PLoS One, 2011. **6**(2): p. e17439.
45. Lindblade, K.A., et al., *The silent threat: asymptomatic parasitemia and malaria transmission*. Expert Rev Anti Infect Ther, 2013. **11**(6): p. 623-39.
46. Okell, L.C., et al., *Factors determining the occurrence of submicroscopic malaria infections and their relevance for control*. Nat Commun, 2012. **3**: p. 1237.
47. Achan, J., et al., *Quinine, an old anti-malarial drug in a modern world: role in the treatment of malaria*. Malar J, 2011. **10**: p. 144.
48. Dondorp, A., et al., *Artesunate versus quinine for treatment of severe falciparum malaria: a randomised trial*. Lancet, 2005. **366**(9487): p. 717-25.
49. WHO, *Guidelines for the Treatment of Malaria*. 2015, World Health Organisation: Geneva.
50. Macdonald, G., *The epidemiology and control of malaria*. 1957, London: Oxford University Press.
51. Bousema, T. and C. Drakeley, *Epidemiology and infectivity of Plasmodium falciparum and Plasmodium vivax gametocytes in relation to malaria control and elimination*. Clin Microbiol Rev, 2011. **24**(2): p. 377-410.
52. Aydin-Schmidt, B., et al., *Usefulness of Plasmodium falciparum-specific rapid diagnostic tests for assessment of parasite clearance and detection of recurrent infections after artemisinin-based combination therapy*. Malar J, 2013. **12**: p. 349.
53. Kyabayinze, D.J., et al., *Operational accuracy and comparative persistent antigenicity of HRP2 rapid diagnostic tests for Plasmodium falciparum malaria in a hyperendemic region of Uganda*. Malar J, 2008. **7**: p. 221.
54. Swarthout, T.D., et al., *Paracheck-Pf accuracy and recently treated Plasmodium falciparum infections: is there a risk of over-diagnosis?* Malar J, 2007. **6**: p. 58.
55. Makanga, M. and S. Krudsood, *The clinical efficacy of artemether/lumefantrine (Coartem)*. Malar J, 2009. **8 Suppl 1**: p. S5.
56. Pasvol, G., *The treatment of complicated and severe malaria*. Br Med Bull, 2005. **75-76**: p. 29-47.
57. Arevalo-Herrera, M., et al., *Plasmodium vivax sporozoite challenge in malaria-naïve and semi-immune Colombian volunteers*. PLoS One, 2014. **9**(6): p. e99754.
58. Cheng, Q., J. Cunningham, and M.L. Gatton, *Systematic review of sub-microscopic P. vivax infections: prevalence and determining factors*. PLoS Negl Trop Dis, 2015. **9**(1): p. e3413.
59. Harris, I., et al., *A large proportion of asymptomatic Plasmodium infections with low and sub-microscopic parasite densities in the low transmission setting of Temotu Province, Solomon Islands: challenges for malaria diagnostics in an elimination setting*. Malar J, 2010. **9**: p. 254.
60. Markell, E.K. and M. Voge, *Medical Parasitology*. Academic Medicine, 1965. **40**(7): p. 719.
61. Yount, E.H., Jr. and L.T. Coggeshall, *Status of immunity following cure of recurrent vivax malaria*. Am J Trop Med Hyg, 1949. **29**(5): p. 701-5.

62. Adolphe, M. *Chemotherapy*. in *Proceedings of the 7th International Congress of Pharmacology*. 1978. Paris: Elsevier.
63. Tripura, R., et al., *Persistent Plasmodium falciparum and Plasmodium vivax infections in a western Cambodian population: implications for prevention, treatment and elimination strategies*. Malaria Journal, 2016. **15**(1): p. 181.
64. Nguyen, T.-N., et al., *The persistence and oscillations of submicroscopic Plasmodium falciparum and Plasmodium vivax infections over time in Vietnam: an open cohort study*. The Lancet Infectious Diseases, 2018. **18**(5): p. 565-572.
65. Naing, C., et al., *Is Plasmodium vivax malaria a severe malaria?: a systematic review and meta-analysis*. PLoS Negl Trop Dis, 2014. **8**(8): p. e3071.
66. Vallejo, A.F., et al., *Plasmodium vivax gametocyte infectivity in sub-microscopic infections*. Malar J, 2016. **15**: p. 48.
67. Rahimi, B.A., et al., *Severe vivax malaria: a systematic review and meta-analysis of clinical studies since 1900*. Malar J, 2014. **13**: p. 481.
68. Barcus, M.J., et al., *Demographic risk factors for severe and fatal vivax and falciparum malaria among hospital admissions in northeastern Indonesian Papua*. Am J Trop Med Hyg, 2007. **77**(5): p. 984-91.
69. Price, R.N., N.M. Douglas, and N.M. Anstey, *New developments in Plasmodium vivax malaria: severe disease and the rise of chloroquine resistance*. Curr Opin Infect Dis, 2009. **22**(5): p. 430-5.
70. Tjitra, E., et al., *Multidrug-resistant Plasmodium vivax associated with severe and fatal malaria: a prospective study in Papua, Indonesia*. PLoS Med, 2008. **5**(6): p. e128.
71. Bharti, A.R., et al., *Experimental infection of the neotropical malaria vector Anopheles darlingi by human patient-derived Plasmodium vivax in the Peruvian Amazon*. Am J Trop Med Hyg, 2006. **75**(4): p. 610-6.
72. Gething, P.W., et al., *Modelling the global constraints of temperature on transmission of Plasmodium falciparum and P. vivax*. Parasit Vectors, 2011. **4**: p. 92.
73. White, M.T., et al., *Modelling the contribution of the hypnozoite reservoir to Plasmodium vivax transmission*. Elife, 2014. **3**.
74. Brasil, P., et al., *Unexpectedly long incubation period of Plasmodium vivax malaria, in the absence of chemoprophylaxis, in patients diagnosed outside the transmission area in Brazil*. Malar J, 2011. **10**: p. 122.
75. Cheoymang, A., et al., *Patients' adherence and clinical effectiveness of a 14-day course of primaquine when given with a 3-day chloroquine in patients with Plasmodium vivax at the Thai-Myanmar border*. Acta Trop, 2015. **152**: p. 151-156.
76. Leslie, T., et al., *Compliance with 14-day primaquine therapy for radical cure of vivax malaria--a randomized placebo-controlled trial comparing unsupervised with supervised treatment*. Trans R Soc Trop Med Hyg, 2004. **98**(3): p. 168-73.
77. Pereira, E.A., E.A. Ishikawa, and C.J. Fontes, *Adherence to Plasmodium vivax malaria treatment in the Brazilian Amazon Region*. Malar J, 2011. **10**: p. 355.
78. Takeuchi, R., et al., *Directly-observed therapy (DOT) for the radical 14-day primaquine treatment of Plasmodium vivax malaria on the Thai-Myanmar border*. Malar J, 2010. **9**: p. 308.
79. Baird, J.K. and S.L. Hoffman, *Primaquine therapy for malaria*. Clin Infect Dis, 2004. **39**(9): p. 1336-45.
80. WHO, *Evidence Review Group meeting report: Point-of-care G6PD testing to support safe use of primaquine for the treatment of vivax malaria*. 2014, World Health Organisation.

81. Douglas, N.M., et al., *Plasmodium vivax* recurrence following falciparum and mixed species malaria: risk factors and effect of antimalarial kinetics. Clin Infect Dis, 2011. **52**(5): p. 612-20.
82. Chu, C.S. and N.J. White, *Management of relapsing Plasmodium vivax malaria*. Expert Rev Anti Infect Ther, 2016. **14**(10): p. 885-900.
83. Cappellini, M.D. and G. Fiorelli, *Glucose-6-phosphate dehydrogenase deficiency*. Lancet, 2008. **371**(9606): p. 64-74.
84. Silal, S.P., et al., *Predicting the impact of border control on malaria transmission: A Simulated Focal Screen and Treat campaign*. In Preparation, 2015.
85. Hendriksen, I.C., et al., *Defining falciparum-malaria-attributable severe febrile illness in moderate-to-high transmission settings on the basis of plasma PfHRP2 concentration*. J Infect Dis, 2013. **207**(2): p. 351-61.
86. Imwong, M., et al., *Numerical Distributions of Parasite Densities During Asymptomatic Malaria*. J Infect Dis, 2016. **213**(8): p. 1322-9.
87. Chourasia, M.K., et al., *Burden of asymptomatic malaria among a tribal population in a forested village of central India: a hidden challenge for malaria control in India*. Public Health, 2017. **147**: p. 92-97.
88. Zaloumis, S., et al., *Assessing the utility of an anti-malarial pharmacokinetic-pharmacodynamic model for aiding drug clinical development*. Malar J, 2012. **11**: p. 303.
89. Branch, O., et al., *Clustered local transmission and asymptomatic Plasmodium falciparum and Plasmodium vivax malaria infections in a recently emerged, hypoendemic Peruvian Amazon community*. Malar J, 2005. **4**: p. 27.
90. Kochar, D.K., et al., *Severe Plasmodium vivax malaria: a report on serial cases from Bikaner in northwestern India*. Am J Trop Med Hyg, 2009. **80**(2): p. 194-8.
91. Starzengruber, P., et al., *High prevalence of asymptomatic malaria in south-eastern Bangladesh*. Malar J, 2014. **13**: p. 16.
92. Grueninger, H. and K. Hamed, *Transitioning from malaria control to elimination: the vital role of ACTs*. Trends Parasitol, 2013. **29**(2): p. 60-4.
93. Hopkins, H., et al., *Highly sensitive detection of malaria parasitemia in a malaria-endemic setting: performance of a new loop-mediated isothermal amplification kit in a remote clinic in Uganda*. J Infect Dis, 2013. **208**(4): p. 645-52.
94. Polley, S.D., et al., *Clinical evaluation of a loop-mediated amplification kit for diagnosis of imported malaria*. J Infect Dis, 2013. **208**(4): p. 637-44.
95. Imwong, M., et al., *High-throughput ultrasensitive molecular techniques for quantifying low-density malaria parasitemias*. J Clin Microbiol, 2014. **52**(9): p. 3303-9.
96. Maude, R.J., et al., *Estimating the burden of clinical malaria over time in the Asia-Pacific*. Wellcome Open Res - in submission, 2018.
97. Riley, J. and R.J. Maude, *Seeking care for malaria and non-specific febrile illness in the Asia-Pacific: a systematic review and meta-analysis*. Wellcome Open Res - in submission, 2018.